Atmospheric
Chemistry
and Physics

Supplement of

Nocturnal atmospheric synergistic oxidation reduces the formation of low-volatility organic compounds from biogenic emissions

Han Zang et al.

Correspondence to: Dandan Huang (huangdd@saes.sh.cn) and Yue Zhao (yuezhao20@sjtu.edu.cn)

S1. Sensitivity analyses on the instrument sensitivities to different compounds

Considering that different compounds could potentially have different CIMS sensitivities, we have conducted a sensitivity analysis by using different instrument sensitivities for different compounds to clarify their influences on the relative changes in RO_2 and HOMs in the $O_3 + NO_3$ regime versus the O_3-only regime. Taking a 10 times higher sensitivity to the compounds with an O/C ratio less than 0.7, the total signals are elevated in both oxidation regimes, but there remain significant decreases in total RO_2 and HOM signals in the synergistic oxidation regime compared to the O_3-only regime (Figure S4a). In addition, given that the sensitivity of nitrate-CIMS to ONs are relatively low, a 10 times higher sensitivity was also considered for the ONs. Under this condition, although ONs make a larger contribution to the total HOM monomers and dimers in the $O_3 + NO_3$ regime (Figure S4b), the signals of both $C_xH_yO_z$ RO_2 and HOMs still decrease significantly due to the presence of NO_3 oxidation. Therefore, different instrument sensitivities to RO_2 and HOMs with different oxygenation levels would not significantly influence the results (e.g., Figure 1 in the main text) in this study.

S2. Sensitivity analyses on the rate constant of the $^{NO3}RO_2 + ^{Cl}RO_2$ reactions

In the present study, a default rate constant of 2×10^{-12} cm^3 molecule^{-1} s^{-1} was chosen for $^{NO3}RO_2 + ^{Cl}RO_2$. Considering that there remains large uncertainty in this rate constant, we have conducted a sensitivity analysis to evaluate its influence on the ratio of k_{NO3+Cl}/k_{NO3+OH}. It should be noted that the self/cross-reaction rate constants of $^{Cl}RO_2$ and $^{OH}RO_2$ are held constant at 2×10^{-12} cm^3 molecule^{-1} s^{-1} (Zhao et al., 2018) in this analysis. As shown in Figure S7, when the $^{NO3}RO_2 + ^{Cl}RO_2$ rate constant increase from $2 \times 10^{-13} - 2 \times 10^{-12}$ cm^3 molecule^{-1} s^{-1}, the best agreements between modelled and measured signal ratios of RO_2 and HOMs are achieved consistently with a k_{NO3+Cl}/ k_{NO3+OH} ratio of $10 - 100$. These results suggest that the uncertainty in the $^{NO3}RO_2 + RO_2$ kinetics would not alter the conclusion regarding the relative reaction efficiency of $^{NO3}RO_2 + ^{Cl}RO_2$ versus $^{NO3}RO_2 + ^{OH}RO_2$.

S3. Sensitivity analyses on the dimer formation branching ratio of RO$_2$ cross reactions

Currently, quantitative constraints on the ROOR dimer formation branching ratio are rather limited. Considering the large uncertainties in this branching ratio, we conducted a sensitivity analysis to evaluate its influence on the relative changes in RO_2 and related HOM concentrations in the synergistic $O_3 + NO_3$ regime versus the O_3-only regime. As shown in Figure S8, as the dimer

formation branching ratio increases from 9% to 50%, the variation in the abundance $C_xH_yO_z$-RO_2 and HOMs due to the concurrence of NO_3 oxidation changes slightly ($< 9\%$ and $< 10\%$, respectively). These results suggest that the uncertainties in the dimer formation branching ratio of RO_2 cross-reactions do not significantly affect the distribution of RO_2 and HOMs across different oxidation regimes.

S4. Model simulations under typical conditions in southeastern United States

A model simulation was also conducted to evaluate the influences of synergistic oxidation on HOM formation under typical nocturnal conditions of the southeastern United States. The constant concentrations of α-pinene (1.5 ppb), isoprene (4.5 ppb), O_3 (30 ppb), NO (20 ppt), NO_2 (2 ppb), NO_3 radicals (1.4 ppt), OH radicals (2.5×10^5 molecules cm^{-3}), and HO_2 radicals (4 ppt) were used according to field observations in this region (Ayres et al., 2015; Lee et al., 2016b). The rate constant of self/cross reactions involving isoprene-derived RO_2 radicals (termed RO_2(isop)) was set to 2×10^{-12} cm^3 molecule^{-1} s^{-1}, with a dimer formation branching ratio of 50% for RO_2(isop) with RO_2 arising from α-pinene (termed RO_2(αp)), and 30% for RO_2(isop) + for RO_2(isop) (Berndt et al., 2018; Wang et al., 2021). In the absence of isoprene, the synergistic $O_3 + NO_3$ oxidation of α-pinene leads to a reduction of 13% and 24% in the formation of $C_xH_yO_z$-HOM monomers and dimers, respectively (Figure S14a). When isoprene is present, as the isoprene + NO_3 oxidation produces a significant amount of nitrooxy RO_2(isop), the synergistic oxidation leads to a slightly larger reduction in $C_xH_yO_z$-HOM monomers and dimers (15% and 31%, respectively, Figure S14b).

Table S1. Summary of conditions and the consumption of α-pinene by each oxidant in different flow tube experiments.

Exp #	α-pinene conc	O_3 conc	NO_2 conc (simulated)	NO_3 conc (simulated)	N_2O_5 conc (simulated)	Cyclohexane conc	Residence time (s)	Total reacted α-pinene	Reacted α-pinene by O_3	Reacted α-pinene by OH	Reacted α-pinene by NO_3
1	100	394	-	-	-	-	25	4.2	2.2	2.0	0
2	200	394	-	-	-	-	25	8.4	4.3	4.0	0
3	300	394	-	-	-	-	25	12.5	6.5	6.0	0
4	400	394	-	-	-	-	25	16.6	8.6	8.0	0
5	500	394	-	-	-	-	25	20.7	10.7	10.0	0
6	100	397	-	-	-	100*1000	25	2.3	2.3	0.02	0
7	100	394	4.5	2.7	11.5	-	25	14.1	2.0	1.8	10.3
8	200	394	4.5	2.7	11.5	-	25	18.4	4.2	3.8	10.4
9	300	394	4.5	2.7	11.5	-	25	22.6	6.3	5.8	10.4
10	400	394	4.5	2.7	11.5	-	25	26.7	8.5	7.8	10.4
11	500	394	4.5	2.7	11.5	-	25	30.8	10.6	9.8	10.4
12	100	397	4.5	2.7	11.5	100*1000	25	12.4	2.1	0.01	10.3
13#	300	270	-	-	-	-	180	54.3	28.9	25.4	0
14#	300	270	6.4	2.3	11.2	-	180	65.4	28.2	23.3	14.0

Note: All species concentrations are in ppb. The initial concentration of α-pinene was estimated according to its gas concentration in the canister and the dilution ratio in the flow tube, the concentration of cyclohexane was derived assuming that the cyclohexane in the gentle flow of ultra-high-purity N_2 bubbled through its liquid was saturated, and the O_3 concentration was measured with an ozone analyzer (T400, API). Exps 1-6 and 7-12 are HOM formation experiments in the O_3-only and O_3 + NO_3 regimes, respectively, and Exps 13 and 14 are SOA formation experiments in the two oxidation regimes.

Table S2. Molecular formula and molar mass of highly oxygenated $^{NO3}RO_2$ and $C_xH_yO_z$-HOM monomers which have very close molar masses.

$^{NO3}RO_2$	molar mass (g mol^{-1})	CHO-HOM	molar mass (g mol^{-1})
C10H16NO6	246.0978	C10H14O7	246.0740
C10H16NO7	262.0927	C10H14O8	262.0689
C10H16NO8	278.0876	C10H14O9	278.0638
C10H16NO9	294.0825	C10H14O10	294.0587
C10H16NO10	310.0774	C10H14O11	310.0536
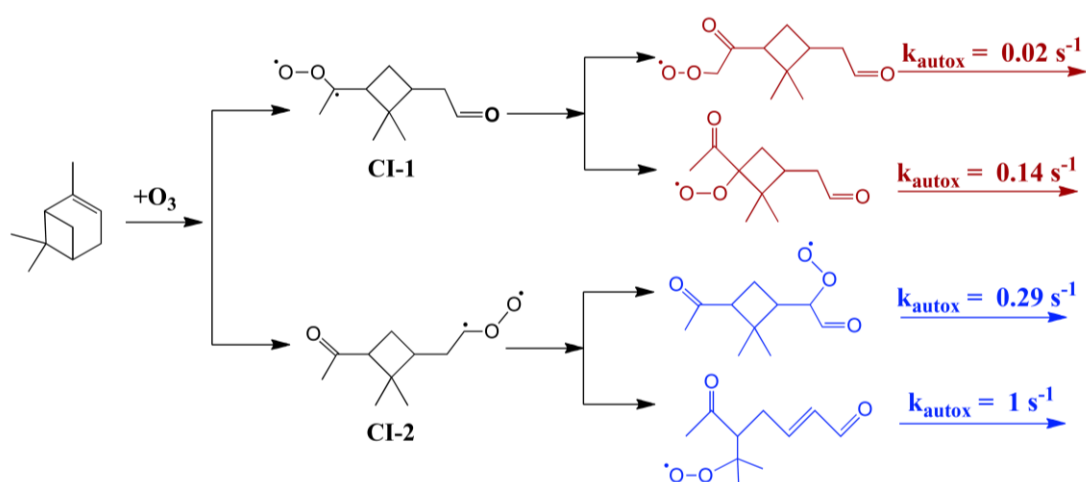
Scheme S1. Simplified pathways leading to the formation of four different primary $^{Cl}RO_2$ radicals.
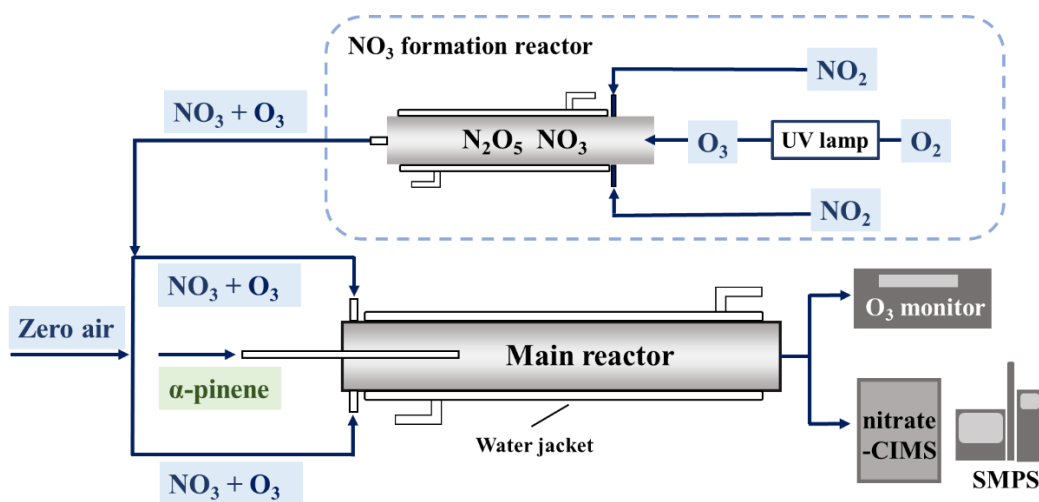
Figure S1. Schematic diagram of the flow tube system used for synergistic oxidation experiments.
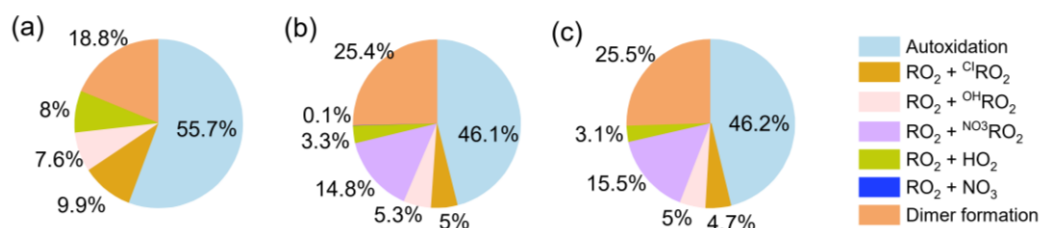
Figure S2. RO$_2$ fates in the (a) O$_3$-only and (b, c) O$_3$ + NO$_3$ regimes, taking C$_{10}$H$_{15}$O$_6$-^{Cl}RO$_2$ in Exps 3 and 9 as an example. The reactions of NO$_3$ + RO$_2$ are considered in (b) but not in (c).
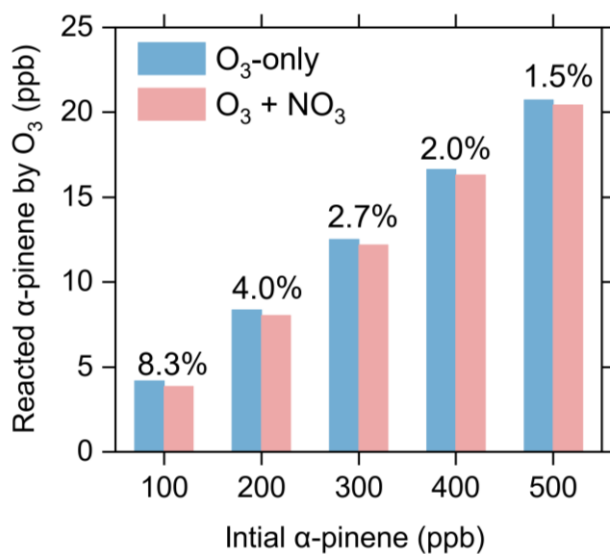

Figure S3. Simulated reacted α-pinene by O$_3$ as a function of initial α-pinene concentrations in O$_3$-only and O$_3$ + NO$_3$ regimes (Exps 1-5, 7-11).
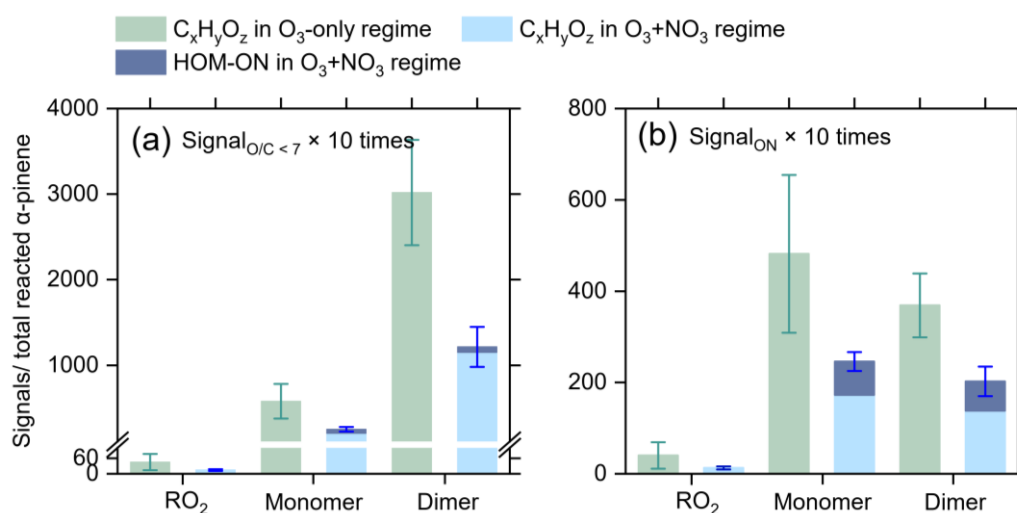

Figure S4. Influences of different instrument sensitivities on the relative changes in RO$_2$ and HOMs in the synergistic oxidation regime versus the O$_3$-only regime. A 10 times higher instrument sensitivity to (a) compounds with O/C < 0.7 and (b) ONs was considered.
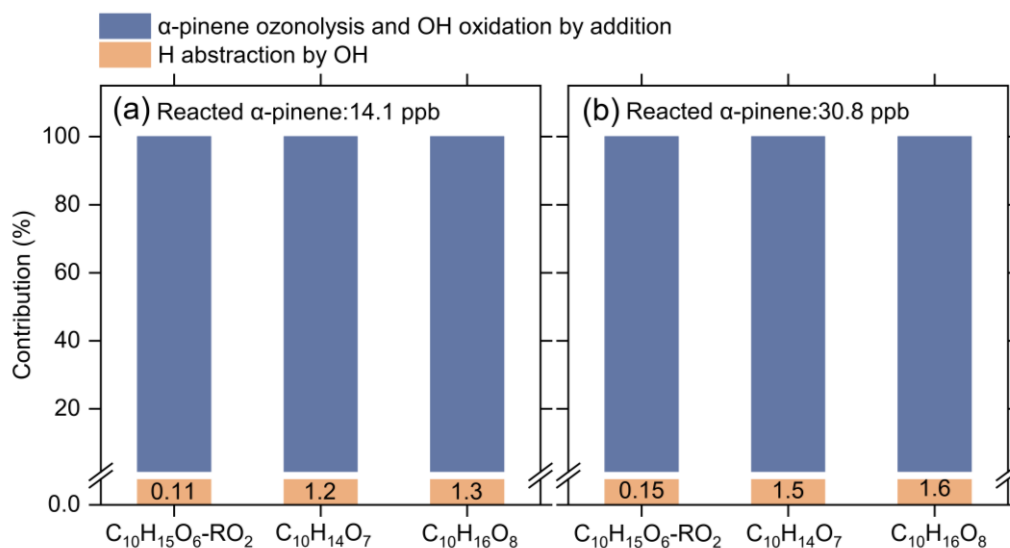
Figure S5. Simulated contributions of the H-abstraction pathways by OH radicals (yellow) and OH-addition and ozonolysis pathways (blue) to the formation of typical RO_2 and HOMs under different reacted α-pinene conditions. The cross-reaction rate constant was set to 2×10^{-13} cm^3 molecule^{-1} s^{-1} for the primary $C_{10}H_{15}O_2$-RO_2 and 2×10^{-12} cm^3 molecule^{-1} s^{-1} for the more oxygenated RO_2. The reaction rate of $RO_2 + NO_3$ is the same as default value in MCM v3.3.1.
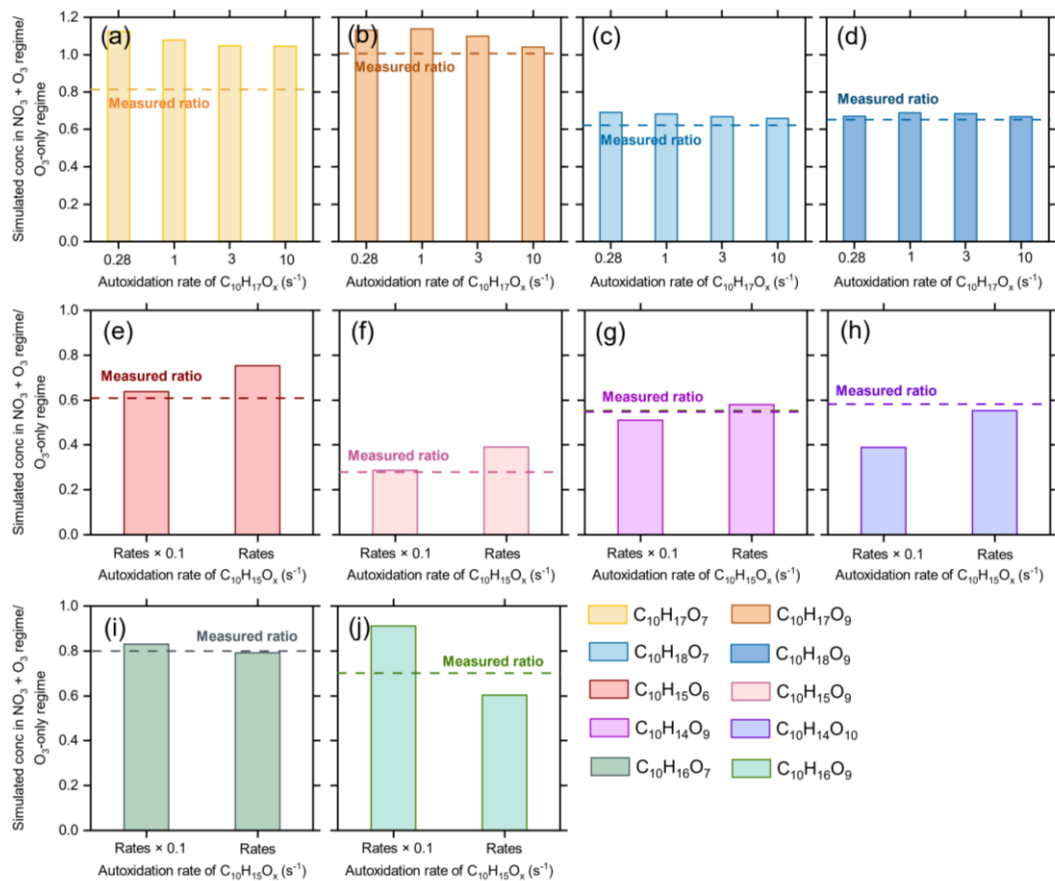
Figure S6. Sensitivity analysis of the autoxidation rate of $^{OH}RO_2$ and $^{Cl}RO_2$. The cross-reaction rates of $^{NO3}RO_2 + {}^{Cl}RO_2$ and $^{NO3}RO_2 + {}^{OH}RO_2$ were set to 2×10^{-12} cm^3 molecule^{-1} s^{-1} and 2×10^{-13} cm^3 molecule^{-1} s^{-1}, respectively, with a dimer formation branching ratio of 50%. The autoxidation rate of $^{OH}RO_2$ varies from $0.28 - 10$ s^{-1}, and the autoxidation rates of the four different $^{Cl}RO_2$ are lowered by a factor of 10.
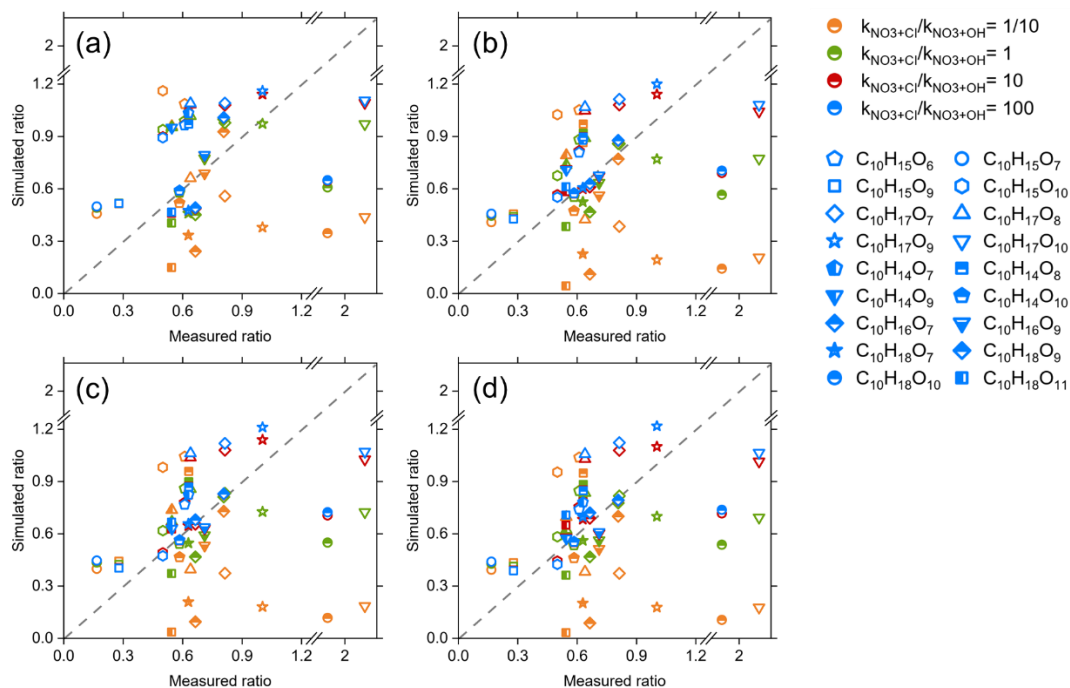
Figure S7. Measurement-model comparisons of the signal ratios of different C_{10} RO_2 and HOMs in the synergistic $O_3 + NO_3$ regime vs. the O_3-only regime. The cross-reaction rate constant of $^{NO3}RO_2 + {}^{Cl}RO_2$ was set to 2×10^{-13} cm^3 molecule^{-1} s^{-1} in (a), 1×10^{-12} cm^3 molecule^{-1} s^{-1} in (b), 1.5×10^{-12} cm^3 molecule^{-1} s^{-1} in (c), 2×10^{-12} cm^3 molecule^{-1} s^{-1} in (d).
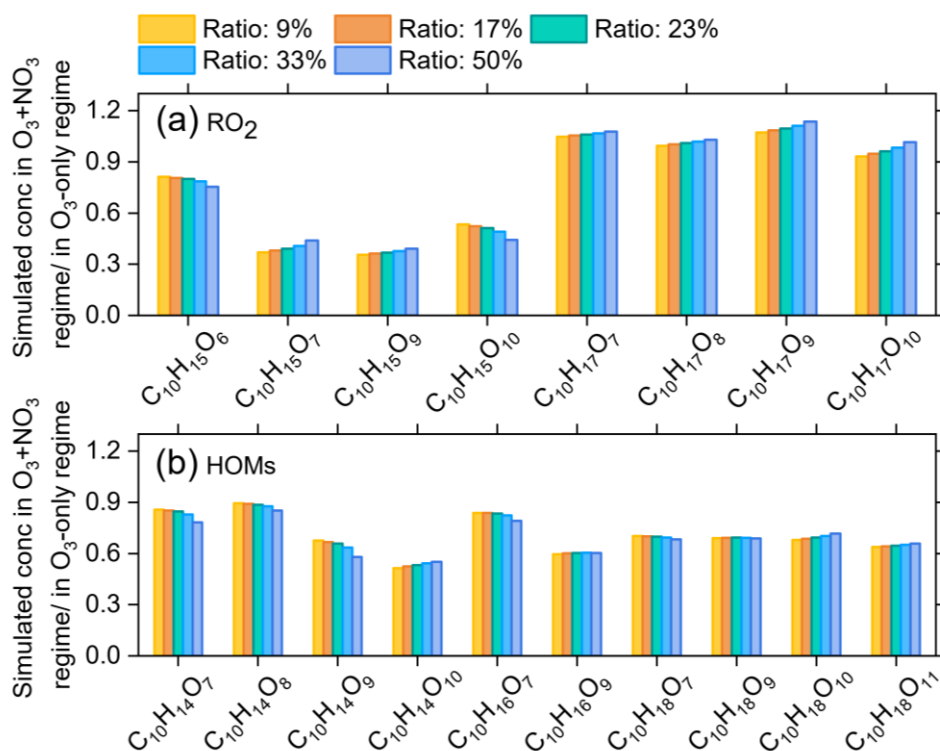

Figure S8. Influences of the dimer formation branching ratio on the relative changes in RO_2 and related HOM concentrations in the synergistic $O_3 + NO_3$ regime vs. the O_3-only regime.
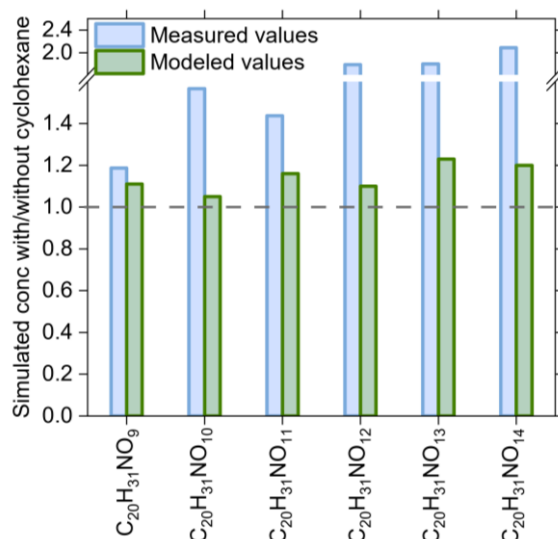
Figure S9. Simulated and measured relative changes in concentrations of $C_{20}H_{31}NO_x$ due to the addition of 100 ppm cyclohexane as an OH scavenger derived in the synergistic $O_3 + NO_3$ regime (Exps 6 and 12).
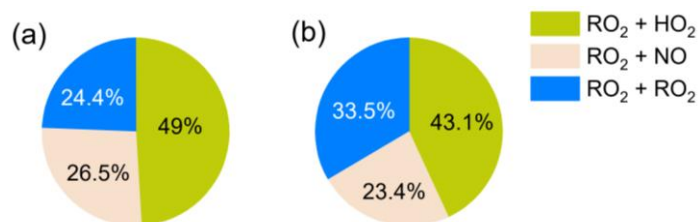

Figure S10. RO_2 fates in the simulations of typical nighttime atmosphere under the condition of low (0.2 ppt, a) and high NO_3 (1 ppt, b) concentrations.
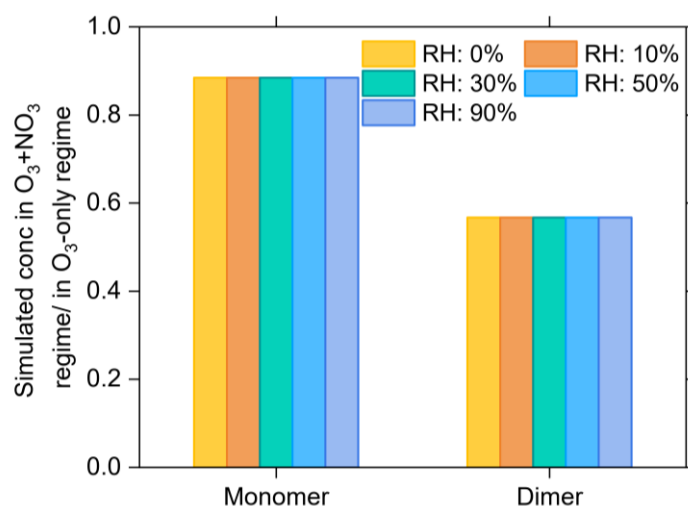

Figure S11. Influence of relative humidity on the relative changes of $C_xH_yO_z$-HOMs in $O_3 + NO_3$ regime compared to those in the O_3-only regime under the typical nocturnal atmospheric conditions.
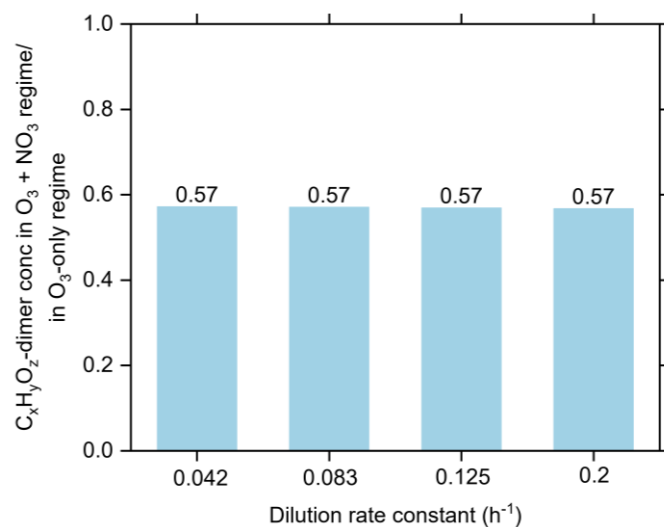
Figure S12. Influence of the dilution rate constant on the reduction of $C_xH_yO_z$-HOM dimers in the $O_3 + NO_3$ synergistic regime.
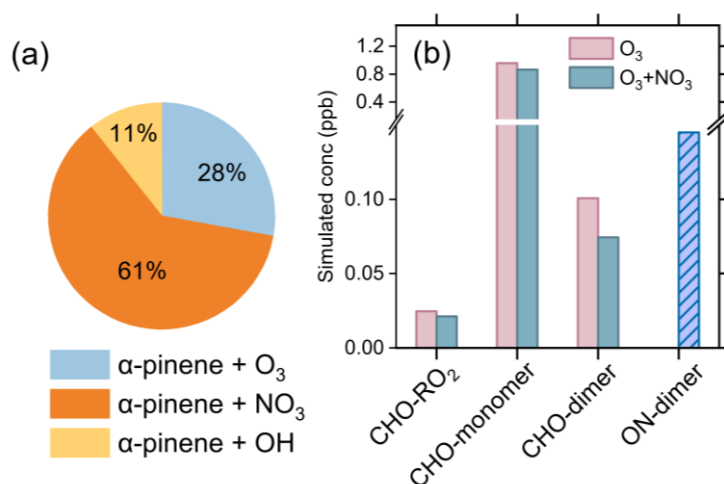

Figure S13. Simulated (a) contributions of different loss pathways of α-pinene by different oxidants and (b) concentrations of $C_xH_yO_z$-HOMs and ONs in the absence and presence of NO_3 radicals under typical nighttime ambient conditions with an OH concentration of 5×10^5 molecules cm^{-3} (Stone et al., 2012; Geyer et al., 2003).
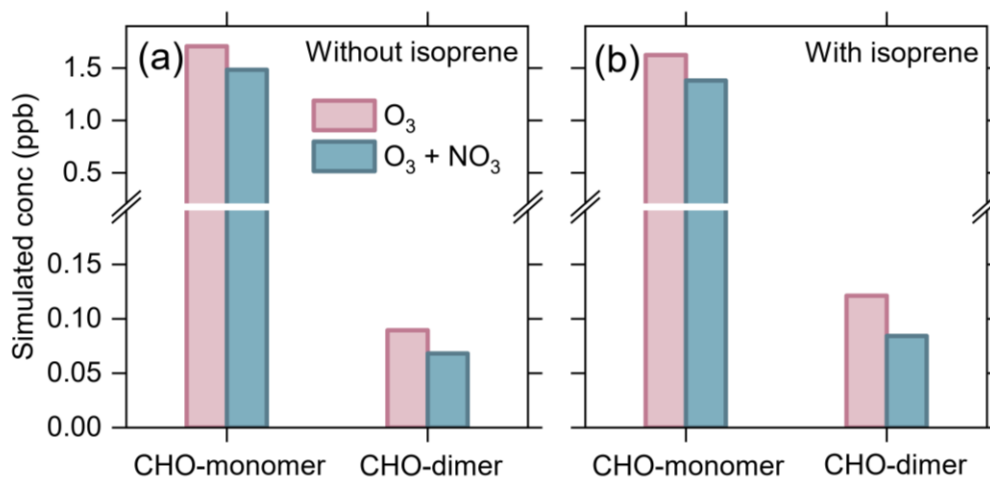
Figure S14. Simulated concentrations of $C_xH_yO_z$-HOMs from the ozonolysis and synergistic O_3 + NO_3 oxidation of α-pinene in the (a) absence and (b) presence of isoprene under typical nocturnal conditions in the southeastern United States.

References:

Berndt, T., Mentler, B., Scholz, W., Fischer, L., Herrmann, H., Kulmala, M., and Hansel, A.: Accretion product formation from ozonolysis and OH radical reaction of alpha-pinene: mechanistic insight and the influence of isoprene and ethylene, Environ. Sci. Technol., 52, 11069-11077, https://doi.org/10.1021/acs.est.8b02210, 2018.

Geyer, A., Bächmann, K., Hofzumahaus, A., Holland, F., Konrad, S., Klüpfel, T., Pätz, H. W., Perner, D., Mihelcic, D., Schäfer, H. J., Volz-Thomas, A., and Platt, U.: Nighttime formation of peroxy and hydroxyl radicals during the BERLIOZ campaign: Observations and modeling studies, J. Geophys. Res.-Atmos., 108, 8249, https://doi.org/10.1029/2001JD000656, 2003.

Stone, D., Whalley, L. K., and Heard, D. E.: Tropospheric OH and HO_2 radicals: field measurements and model comparisons, Chem. Soc. Rev., 41, 6348-6404, https://doi.org/10.1039/c2cs35140d, 2012.

Wang, Y., Zhao, Y., Li, Z., Li, C., Yan, N., and Xiao, H.: Importance of hydroxyl radical chemistry in isoprene suppression of particle formation from α-pinene ozonolysis, ACS Earth Space Chem., 5, 487-499, https://doi.org/10.1021/acsearthspacechem.0c00294, 2021.

Zhao, Y., Thornton, J. A., and Pye, H. O. T.: Quantitative constraints on autoxidation and dimer formation from direct probing of monoterpene-derived peroxy radical chemistry, P. Natl. Acad. Sci. USA, 115, 12142-12147, https://doi.org/10.1073/pnas.1812147115, 2018.